Phase-Tuned Tetrapod-Shaped CdTe Nanocrystals by Ligand Effect

Jin Woo Cho, Han Sung Kim, Yun Ju Kim, So Young Jang, and Jeunghee Park*

Department of Chemistry, Korea University, Jochiwon 339-700, Korea

Jin-Gyu Kim and Youn-Joong Kim

Division of Electron Microscopic Research, Korea Basic Research Institute, Daejon 305-333, Korea

Eun Hee Cha

Department of Liberal Art and Literature, Hoseo University, Asan Chungnam 336-795, Korea

Received May 19, 2008. Revised Manuscript Received June 26, 2008

We achieved extensive control of the morphology and phase of colloidal cadmium telluride (CdTe) nanocrystals (NCs) using two different types of capping ligands, namely, amines and phosphonic acids having various alkyl chains ranging from butyl (C4) to octadecyl (C18). Among the alkylamines, the largest tetrapods are preferentially produced using octylamine (C8), suggesting that the steric hindrance of the alkyl chains optimizes the growth condition of the tetrapods. The phase of the tetrapod branches can be tuned from wurtzite to zinc blende by enhancing the steric hindrance of the tertiary alkyl phosphine used as the Te activating ligand. The in situ synthesis of tetrapod CdTe NCs on carbon nanotubes (CNTs) was performed using the two types of ligands. All of the CdTe NCs grown on the CNTs consisted of wurtzite phase, and the largest tetrapods are produced using phosphonic acid having the alkyl chain, C10.

1. Introduction

As one of the important colloidal wide-band gap II−VI semiconductor nanomaterials, CdTe (bulk $E_g = 1.44$ eV at 300 K) nanocrystals (NCs) are of great interest for both fundamental studies and various promising applications in the field of photonic crystals, light-emitting diodes (LEDs), solar cells, and bioimaging.[1−6] They usually exhibit distinctive optical and electronic properties, which are strongly dependent on their size and shape (i.e., quantum size effects) and which are distinctive from those of the corresponding bulk counterparts. Therefore, the control of the size and shape of NCs has been the most significant issue and has advanced dramatically in the past few years.[1−3,7−9] Among the various nanostructures, tetrapod-shaped CdTe NCs have received a tremendous amount of attention, due to their unique optical/mechanical properties.[10−20] However, developing an improved synthesis method that increases the yield of nanostructures with this shape and controls the crystal phase (wurtzite and zinc blende) still remains quite a challenge.

Recently, significant interest has been directed toward the design of NC (e.g., CdS, CdSe, CdTe, ZnS, ZnSe, PbS, PbSe, Cu_2S) and carbon nanotube (CNT) hybrid nanostructures, to extend the range of applications.[21−28] In particular, CdTe NC−CNT hybrid nanostructures allow for the highly efficient generation of photocurrents via the interaction between the excited semiconductor NCs and the conductive CNTs, thus demonstrating their importance as building blocks for light harvesting assemblies.[23] However, the size and morphology

* Corresponding author. E-mail: parkjh@korea.ac.kr.

(1) Murray, C. B.; Norris, D. J.; Bawendi, M. G. *J. Am. Chem. Soc.* **1993**, *115*, 8706.
(2) Peng, Z. A.; Peng, X. *J. Am. Chem. Soc.* **2001**, *123*, 183.
(3) Tang, Z.; Kotov, N. A.; Giersig, M. *Science* **2002**, *297*, 237.
(4) (a) Rogach, A.; Susha, A.; Caruso, F.; Sukhorukov, G.; Kornowski, A.; Kershaw, S.; Möhwald, H.; Eychmüller, A; Weller, H. *Adv. Mater.* **2000**, *12*, 333. (b) Gao, M.; Lesser, C.; Kristein, S.; Möhwald, H.; Rogach, A. L.; Weller, H. *J. Appl. Phys.* **2000**, *87*, 2297.
(5) Gur, I.; Fromer, N. A.; Geier, M. L.; Alivisatos, A. P. *Science* **2005**, *310*, 462.
(6) (a) Mamedova, N. N.; Kotov, N. A.; Rogach, A. L.; Studer, J. *Nano Lett.* **2001**, *1*, 281. (b) Michalet, X.; Pinaud, F. F.; Bentolila, L. A.; Tsay, J. M.; Doose, S.; Li, J. J.; Sundaresan, G.; Wu, A. M.; Gambhir, S. S.; Weiss, S. *Science* **2005**, *307*, 538. (c) Lee, J.; Hernandez, P.; Lee, J.; Govorov, A. O.; Kotov, N. A. *Nat. Mater.* **2007**, *6*, 291.
(7) Peng, X. *Adv. Mater.* **2003**, *15*, 459.
(8) Kumar, S.; Nann, T. *Small* **2006**, *2*, 316.
(9) Jun, Y.; Choi, J.; Cheon, J. *Angew. Chem., Int. Ed.* **2006**, *45*, 3414.
(10) (a) Manna, L.; Milliron, D. J.; Meisel, A.; Scher, E. C.; Alivisatos, A. P. *Nat. Mater.* **2003**, *2*, 382. (b) Milliron, D. J.; Hughes, S. M.; Cui, Y.; Manna, L.; Li, J.; Wang, L. W.; Alivisatos, A. P. *Nature* **2004**, *430*, 190. (c) Liu, H.; Alivisatos, A. P. *Nano Lett.* **2004**, *4*, 2397.
(11) Bunge, S. D.; Krueger, K. M.; Boyle, T. J.; Rodriguez, M. A.; Headley, T. J.; Colvin, V. L. *J. Mater. Chem.* **2003**, *13*, 1705.
(12) Yu, W. W.; Wang, Y. A.; Peng, X. *Chem. Mater.* **2003**, *15*, 4300.
(13) Peng, P.; Milliron, D. J.; Hughes, S. M.; Johnson, J. C.; Alivisatos, A. P.; Saykally, R. J. *Nano Lett.* **2005**, *5*, 1809.
(14) Zhang, J.-Y.; Yu, W. W. *Appl. Phys. Lett.* **2006**, *89*, 123108.
(15) Carbone, L.; Kudera, S.; Carlino, E.; Parak, W. J.; Giannini, C.; Cingolani, R.; Manna, L. *J. Am. Chem. Soc.* **2006**, *128*, 748.
(16) Li, Y.; Zhong, H.; Li, R.; Zhou, Y.; Yang, C.; Li, Y. *Adv. Funct. Mater.* **2006**, *16*, 1705.
(17) Tari, D.; De Giorgi, M.; Della Sala, F.; Carbone, L.; Krahne, R.; Manna, L.; Cingolani, R.; Kudera, S.; Parak, W. J. *Appl. Phys. Lett.* **2005**, *87*, 224101.
(18) Krahne, R.; Chilla, G.; Schueller, C.; Carbone, L.; Kudera, S.; Mannarini, G.; Manna, L.; Heitmann, D.; Cingolani, R. *Nano Lett.* **2006**, *6*, 478.
(19) Malkmus, S.; Kudera, S.; Manna, L.; Parak, W. J.; Braun, M. *J. Phys. Chem. B* **2006**, *110*, 17334.
(20) Fang, L.; Park, J. Y.; Cui, Y.; Alivisatos, A. P.; Shcrier, J.; Lee, B.; Wang, L.-W.; Salmeron, M. *J. Chem. Phys.* **2007**, *127*, 184704.

10.1021/cm801359k CCC: $40.75
Published on Web 08/06/2008

control of CdTe NCs in the CNT hybrid nanostructure system has not been much investigated yet.

Herein, we report the synthesis of CdTe tetrapods with well-controlled shape /phase/dimensional uniformity through the novel use of the steric effect of the capping ligands. By adopting the well-developed synthetic procedure of the Peng group,[12] we added the following alkyl-chained amines as coordinating coligands in the noncoordinating solvent, 1-octadecene (ODE), namely, butylamine (BA), octylamine (OA), dodecylamine (DDA), tetradecylamine (TDA), octadecylamine (ODA), dioctylamine (DOA), and trioctylamine (TOA). They can act as "sufficient" protection ligands, which can control the shape of the monodispersed NCs. The CdTe NCs exhibit remarkable shape evolution from dots to tetrapods when the length of the alkyl chains of the amines is altered. Remarkably, for the first time, the phase of the tetrapods was able to be controlled from wurtzite to zinc blende structures by changing the Te activating ligands from tributylphosphine (TBP) to trioctylphosphine (TOP), which form the Te:TBP or Te:TOP complex, respectively.

Furthermore, an in situ synthetic route to prepare CdTe NC and CNT hybrid nanostructures was developed, to show the unique morphology evolution of CdTe tetrapod NCs on the surface of multiwalled CNTs (MWCNTs) and single-walled CNTs (SWCNTs). We used various alkyl-chained phosphonic acids as activating agents for the Cd precursors and coordinating ligands; that is, hexylphosphonic acid (HPA), decylphosphonic acid (DPA), tetradecylphosphonic acid (TDPA), and octadecylphosphonic acid (ODPA). For these dispersed and attached CdTe NCs (on the CNTs), the tetrapod morphology is directly correlated with the alkyl chain length of the amines and phosphonic acids.

2. Experimental Section

Materials. 1-Octadecene (ODE, $C_{17}H_{34}$═CH_2, 90%), cadmium oxide (CdO, 99%), tellurium (Te) powders (99.8%), oleic acid (OLA, C_8H_{16}═C_8H_{15}—COOH, 99%), tributylphosphine (TBP, 97%), trioctylphosphine (TOP, 90%), tri-*n*-octylphosphine oxide (TOPO, 90%), butylamine (BA, *n*-$C_4H_9NH_2$, 99%), octylamine (OA, *n*-$C_8H_{17}NH_2$, 99%), dodecylamine (DDA, *n*-$C_{12}H_{25}NH_2$, 98%), tetradecylamine (TDA, *n*-$C_{14}H_{29}NH_2$, 95%), hexadecylamine (HDA, *n*-$C_{14}H_{29}NH_2$, 98%), octadecylamine (ODA, *n*-$C_{18}H_{37}NH_2$, 97%), dioctylamine (DOA, $(C_8H_{17})_2NH$, 98%), and trioctylamine (TOA, $(C_8H_{17})_3N$, 98%) were purchased from Aldrich. Hexylphosphonic acid (HPA, $C_6H_{13}P(O)(OH)_2$), decylphosphonic acid (DPA, $C_{10}H_{21}P(O)(OH)_2$, 98%), tetradecylphosphonic acid (TDPA, $C_{14}H_{29}P(O)(OH)_2$, 98%), and octadecylphosphonic acid (ODPA, $C_{18}H_{37}P(O)(OH)_2$) were purchased from Alfa. All chemicals were used without further purification. Purified single-walled CNTs (Iljin, 99%) and multiwalled CNTs (Aldrich, ≥95%) were used.

Typical Synthesis of Dispersed CdTe NCs. The procedure was divided into three steps. (1) CdO (0.1 mmol, 12.8 mg) and OLA (0.35 mmol, 0.11 mL) were mixed with 5.0 mL of ODE in a 50 mL three-neck flask equipped with a condenser, and the mixture was heated to 300 °C under argon flow. (2) A solution of Te (0.05 mmol, 6.38 mg) dissolved in 0.13 mL (0.28 mmol) of TOP (or TBP) was swiftly injected into the heated solution, and the reaction mixture was then cooled to 260 °C. (3) The mixture was maintained at 260 °C for 10 min to allow for the growth of the CdTe NCs. For the addition of amines, 0.2 mmol of BA (or OA, DDA, TDA, ODA, HDA, ODA, DOA, TOA) was dissolved in the Te-TOP solution and injected into the hot solution, in the step (2). The other reaction conditions were kept the same as those described above. The molar ratio of precursors and ligands is CdO:Te:OLA:TBP (or TOP): amine = 1:0.5:3.5:2.8:2.

Typical Synthesis of CdTe NCs Attached on CNTs. Two procedures were developed. Method 1: The three steps described above were used. In step (1), 5 mg of SWCNTs or MWCNTs was mixed with CdO and OA. All of the other procedures are identical. Method 2: The procedure was also divided into three steps. (1) 0.1 mmol (12.8 mg) of CdO, 0.16 mmol of HPA (or DPA, TDPA, ODPA), and 5 mg of SWCNTs (or MWCNTs) were dissolved in 2.0 mmol (0.7 g) of TOPO. (2) A solution of 0.1 mmol (12.7 mg) of Te dissolved in 1.0 mmol (0.45 mL) of TOP was swiftly injected into the heated solution (300 °C), and the reaction mixture was immediately cooled to 270 °C. Alternatively, the multi-injection (usually three times) of the Te/TOP solution was performed at the growth temperature. (3) The mixture was maintained at 270 °C for 10 min to allow for the growth of the CdTe NCs on the CNTs.

After the reaction mixture had cooled to approximately 40 °C, the purification of the nanocrystals was carried out by repeatedly extracting the unreacted precursors from the reaction mixture dissolved in hexane by adding methanol, and the CdTe NCs were isolated by precipitation with acetone.

Characterization. The products were characterized by field-emission transmission electron microscopy (FE TEM, FEI TECNAI G2 200 kV and Jeol JEM 2100F) and high-voltage TEM (HVEM, Jeol JEM ARM 1300S, 1.25 MV). High-resolution X-ray diffraction (XRD) patterns were obtained using the 8C2 beam line of the Pohang Light Source (PLS) with monochromatic radiation (λ = 1.54520 Å) and the Cu Kα line (λ = 1.5406 Å) of a laboratory-based diffractometer (Philips X'Pert PRO MRD). X-ray photoelectron spectroscopy (XPS) measurements were performed at the U7

(21) (a) Shi, J.; Qin, Y.; Wu, W.; Li, X.; Guo, Z. -X.; Zhu, D. *Carbon* **2004**, *42*, 423. (b) Huang, Q.; Gao, L. *Nanotechnology* **2004**, *15*, 1855. (c) Sheeney-Haj-Ichia, L.; Basnar, B.; Willner, I. *Angew. Chem., Int. Ed.* **2005**, *44*, 78. (d) Robel, I.; Bunker, B. A.; Kamat, P. V. *Adv. Mater.* **2005**, *17*, 2458. (e) Liu, B.; Lee, J. Y. *J. Phys. Chem. B* **2005**, *109*, 23783. (f) Li, X.; Liu, Y.; Fu, L.; Cao, L.; Wei, D.; Wang, Y. *Adv. Funct. Mater.* **2006**, *16*, 2431. (g) Pan, B.; Cui, D.; Ozkan, C. S.; Ozkan, M.; Xu, P.; Huang, T.; Liu, F.; Chen, H.; Li, Q.; He, R.; Gao, F. *J. Phys. Chem. C* **2008**, *112*, 939.

(22) (a) Banerjee, S.; Wong, S. S. *Nano Lett.* **2002**, *2*, 195. (b) Haremza, J. M.; Hahn, M. A.; Krauss, T. D.; Chen, S.; Calcines, J. *Nano Lett.* **2002**, *2*, 1253. (c) Chaudhary, S.; Kim, J. H.; Singh, K. V.; Ozkan, M. *Nano Lett.* **2004**, *4*, 2415. (d) Landi, B. J.; Castro, S. L.; Ruf, H. J.; Evans, C. M.; Bailey, S. G.; Raffaelle, R. P. *Sol. Energy Mater. Sol. Cells* **2005**, *87*, 733. (e) Li, Q.; Sun, B.; Kinloch, I. A.; Zhi, D.; Sirringhaus, H.; Windle, A. H. *Chem. Mater.* **2006**, *18*, 164. (f) Juarez, B. H.; Klinke, C.; Kornowski, A.; Weller, H. *Nano Lett.* **2007**, *7*, 3564.

(23) (a) Banerjee, S.; Wong, S. S. *J. Am. Chem. Soc.* **2003**, *125*, 10342. (b) Banerjee, S.; Wong, S. S. *Adv. Mater.* **2004**, *16*, 34. (c) Guldi, D. M.; Aminur Rahman, G. M.; Sgobba, V.; Kotov, N. A.; Bonifazi, D.; Prato, M. *J. Am. Chem. Soc.* **2006**, *128*, 2315. (d) Grzelczak, M.; Correa-Duarte, M. A.; Salgueiriño-Maceira, V.; Giersig, M.; Diaz, R.; Liz-Marzán, L. M. *Adv. Mater.* **2006**, *18*, 415. (e) Li, W.; Gao, C.; Qian, H.; Yan, D. *J. Mater. Chem.* **2006**, *16*, 1852. (f) Engtrakul, C.; Kim, Y. -H.; Nedeljkovic, J. M.; Ahrenkiel, S. P.; Gilbert, K. E. H.; Alleman, J. L.; Zhang, S. B.; Micic, O. I.; Nozik, A. J.; Heben, M. J *J. Phys. Chem. B* **2006**, *110*, 25153. (g) Jia, N.; Lian, Q.; Shen, H.; Wang, C.; Li, X.; Yang, Z. *Nano Lett.* **2007**, *7*, 2976.

(24) (a) Kim, H.; Sigmund, W. *J. Cryst. Growth* **2003**, *255*, 114. (b) Du, J.; Fu, L.; Liu, Z.; Han, B.; Li, Z.; Liu, Y.; Sun, Z.; Zhu, D. *J. Phys. Chem. B* **2005**, *109*, 12772. (c) Shan, Y.; Gao, L. *J. Am. Ceram. Soc.* **2006**, *89*, 759. (d) Gu, F.; Li, C.; Wang, S. *Inorg. Chem.* **2007**, *46*, 5343.

(25) Li, B.; Xie, Y.; Xu, Y.; Wu, C.; Zhao, Q. *J. Phys. Chem. B* **2006**, *110*, 14186.

(26) Yu, D.; Chen, Y.; Li, B.; Chen, X.; Zhang, M. *Appl. Phys. Lett.* **2007**, *90*, 161103.

(27) Cho, N.; Choudhury, K. R.; Thapa, R. B.; Sahoo, Y.; Ohulchanskyy, T.; Cartwright, A. N.; Lee, K. S.; Prasad, P. N. *Adv. Mater.* **2007**, *19*, 232.

Table 1. Growth Condition and Shape/Size/Phase of the CdTe NCs, Synthesized in This Study

NC	phosphine[a]	amines	shape	phase[b]	average size of branches[c] (nm)	
					D	*L*
1	TBP		dot	zb	6 ± 0.3	
2		BA (C4)	branched[d] (aggregated)[e]	wz	5 ± 0.5	10 ± 2
3		OA (C8) and DDA (C12)	tetrapod	wz	5 ± 0.5	15 ± 1
4		TDA (C14)	branched	wz	5 ± 0.5	8 ± 1
5		HDA (C16)	branched	wz	4 ± 0.3	5 ± 1
6		ODA (C18)	dot	wz	6 ± 0.5	
7		DOA (2 × C8)	branched	wz	3 ± 0.3	5 ± 1
8		TOA (3 × C8)	branched	wz	3 ± 0.3	4 ± 1
9	TOP		branched	zb	5 ± 0.5	6 ± 1
10		BA (C4)	branched (aggregated)[e]	zb	5 ± 0.5	10 ± 2
11		OA (C8)	tetrapod	zb	5 ± 0.5	25 ± 2
12		DDA (C12)	tetrapod	zb	5 ± 0.5	15 ± 1
13		ODA (C18)	branched	zb	5 ± 0.5	7 ± 1
14		TOA (3 × C8)	branched	zb	5 ± 0.5	7 ± 1

[a] The molar ratio of reactants and ligands is CdO:Te:OLA:TBP (or TOP):aine = 1:0.5:3.5:2.8:2. The same ratio is used for TBP and TOP. [b] The phase of branches is indicated; wz = wurtzite, zb = zinc blende. [c] The average size of branches; *D* = diameter, *L* = length. In the case of dots, *D* is the diameter. [d] Branched structure means a mixture of various shaped multipods with 2−4 short branches. [e] CdTe NCs are produced as aggregated form.

beam line of the PLS and using a laboratory-based spectrometer (XPS, ESCALAB 250, VG Scientifics) with a photon energy of 1486.6 eV (Al Kα). Raman spectroscopy (Horiba Jobin-Yvon HR-800 UV) was measured using the 514.5 nm line of an argon ion laser. UV−visible spectroscopy (Scinco S-3100) was used to identify the growth of the CdTe NCs. Steady-state photoluminescence (PL) measurements were carried out using an He−Cd laser ($\lambda = 325$ nm) as the excitation source. The laser power was below 1 MW/cm^2.

3. Results and Discussions

3.1. Shape Evolution of the Morphology Using Amines. The growth condition and shape/size of the CdTe NCs are listed in Table 1. Figure 1a displays the TEM image of the dot-shaped CdTe NCs (NC1) synthesized without using amines. The avgerage size is 6 ± 0.3 nm. Figure 1b−h displays the TEM images of the CdTe NCs, synthesized using BA, OA (or DDA), TDA, HDA, ODA, DOA, and TOA, respectively. The respective NCs are denoted as NC2−NC8. The ratio of Cd:Te:amine was 1:0.5:2. The amines served as coligands along with TBP and OLA in ODE solvent. When the shortest primary alkyl-chained BA (C4) was added, branched NCs (NC2), that is, a mixture of short elongated structures such as dipods, tripods, and tetrapods, were produced as aggregated forms, as shown in Figure 1b. The average diameter (*D*) of the branches is 5 ± 0.5 nm, and their average length (*L*) is 10 ± 2 nm (inset). When the longer alkyl-chained OA (C8) and DDA (C12) were used, perfect tetrapod-shaped NCs (NC3) were produced in dispersed form (Figure 1c). The branch has average values of $D = 5 \pm 0.5$ nm and $L = 15 \pm 1$ nm. When TDA (C14) was added, branched NCs (NC4) were again produced (Figure 1d). The diameter is $D = 5 \pm 0.5$ nm, but the length decreased to $L = 8 \pm 1$ nm. When the longer alkyl-chained HDA (C16) was added, shorter branched NCs (NC5) with $D = 4 \pm 0.3$ nm and $L = 5 \pm 1$ nm were formed (Figure 1e). The addition of the ODA (C18) produced edged nanodots (NC6) with an average size of 6 ± 0.5 nm, as shown in Figure 1f. Figure 1g,h corresponds to the NCs synthesized using the secondary and tertiary octyl amines DOA (2 × C8) and TOA (3 × C8), respectively. When DOA and TOA was added, branched structures (NC7 and NC8; $D = 3 \pm 0.3$ nm) were produced, respectively, with $L = 5 \pm 1$ and 4 ± 1 nm. Using the HRTEM and XRD data, we found that all of these NCs consisted of a wurtzite phase, when both TBP and amine are used. We referred to wurtzite structure CdTe as "wz-CdTe".

When TOP is used instead of TBP, the more elongated shape becomes dominant. Figure 2a shows the CdTe NCs (NC9) synthesized using only OLA without amines. The NCs exhibit branched structures with the average size of the branches being $D = 5 \pm 0.5$ nm and $L = 6 \pm 1$ nm. When BA was added, the branched NCs (NC10) were produced in an aggregated form, as shown in Figure 2b. Their average size is $D = 5 \pm 0.5$ nm and $L = 10 \pm 2$ nm (inset). Figure 2c displays the TEM images of the tetrapod-shaped CdTe NCs (NC11) synthesized using OA. The inset corresponds to the magnified image of an individual tetrapod, showing their larger average size; $D = 5 \pm 0.5$ nm and $L = 25 \pm 2$ nm. When the longer alkyl-chain DDA (C12) was added, shorter tetrapod-shaped CdTe NCs (NC12) were grown, as shown in Figure 2d. Their average size is reduced to $D = 5 \pm 0.5$ nm and $L = 15 \pm 1$ nm. Figure 2e,f displays the TEM image of the short branched CdTe NCs (NC13 and NC14; $D = 5 \pm 0.5$ nm and $L = 7 \pm 1$ nm) synthesized using ODA and TOA, respectively. The HRTEM and XRD measurement show the formation of zb-CdTe branches (further referred to as "zb-CdTe"), when both TOP and amines are used. The two series of experiments indicate that OA is the most effective in producing the tetrapod structures with the longest branches. The shorter or longer alkyl chained amines shift the morphology from tetrapod to dot shapes by reducing the length of the branches. As the number of octyl chains increases, the tetrapods also evolve into the shorter-branched structures.

3.2. In Situ Growth of Tetrapod-Shaped CdTe NCs on CNTs. The growth conditions and shapes/sizes of the CdTe NCs are listed in Table 2. We performed the synthesis of the attached CdTe NCs on the SWCNTs or MWCNTs. Figure 3a shows the TEM image for the dot-shaped NCs (NC15) decorated over the whole MWCNTs, synthesized without amines (same growth condition as that of NC9). Their average

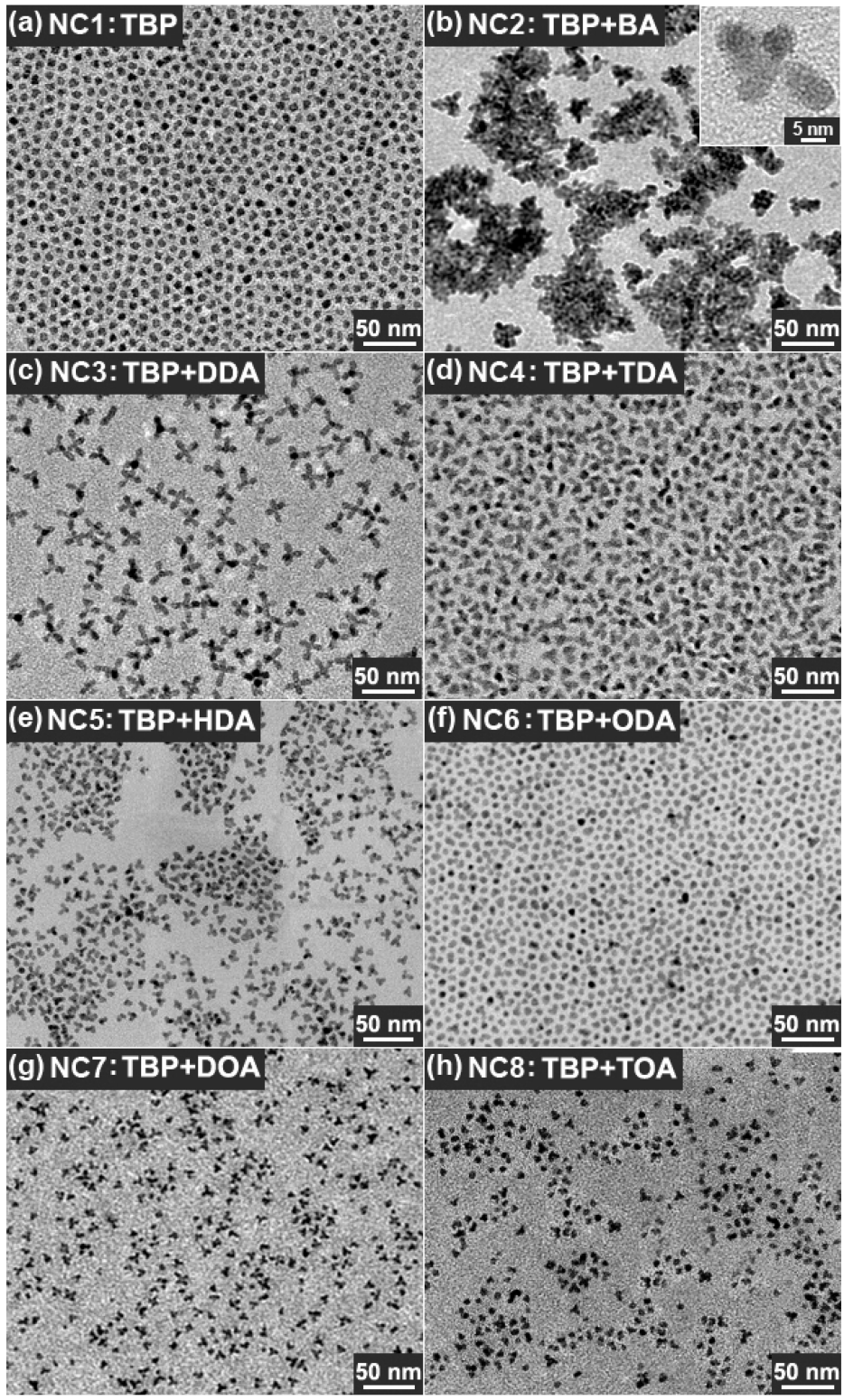

Figure 1. TEM images of CdTe NCs grown using TBP and (a) no amine (NC1), (b) BA (NC2), (c) OA (NC3), (d) TDA (NC4), (e) HDA (NC5), (f) ODA (NC6), (g) DOA (NC7), and (h) TOA (NC8).

size is 5 ± 0.5 nm. When OA was added (same growth condition as that of NC11), tetrapod-shaped CdTe NCs (NC16) were synthesized, as shown in Figure 3b. Their average size is $D = 5 \pm 0.5$ nm and $L = 12 \pm 2$ nm. In the case of the growth of CdTe NCs on the CNTs, the same morphology evolution was observed, which depends on the alkyl chain of the amines. Using the HRTEM and XRD data, we found that all of the NCs attached on the CNTs consisted of a wz-CdTe structure.

The in situ growth of CdTe NCs on the CNTs was performed using phosphonic acid and TOPO instead OLA and ODE, respectively. The TEM image of the CdTe-SWCNT nanostructures (NC17), synthesized using HPA (C6), is displayed in Figure 3c. The SWCNTs are decorated with the branched CdTe NCs. Their average size is $D = 4$

(28) Lee, H. J.; Yoon, S. W.; Kim, Y. J.; Park, J. *Nano Lett.* **2007**, *7*, 778.

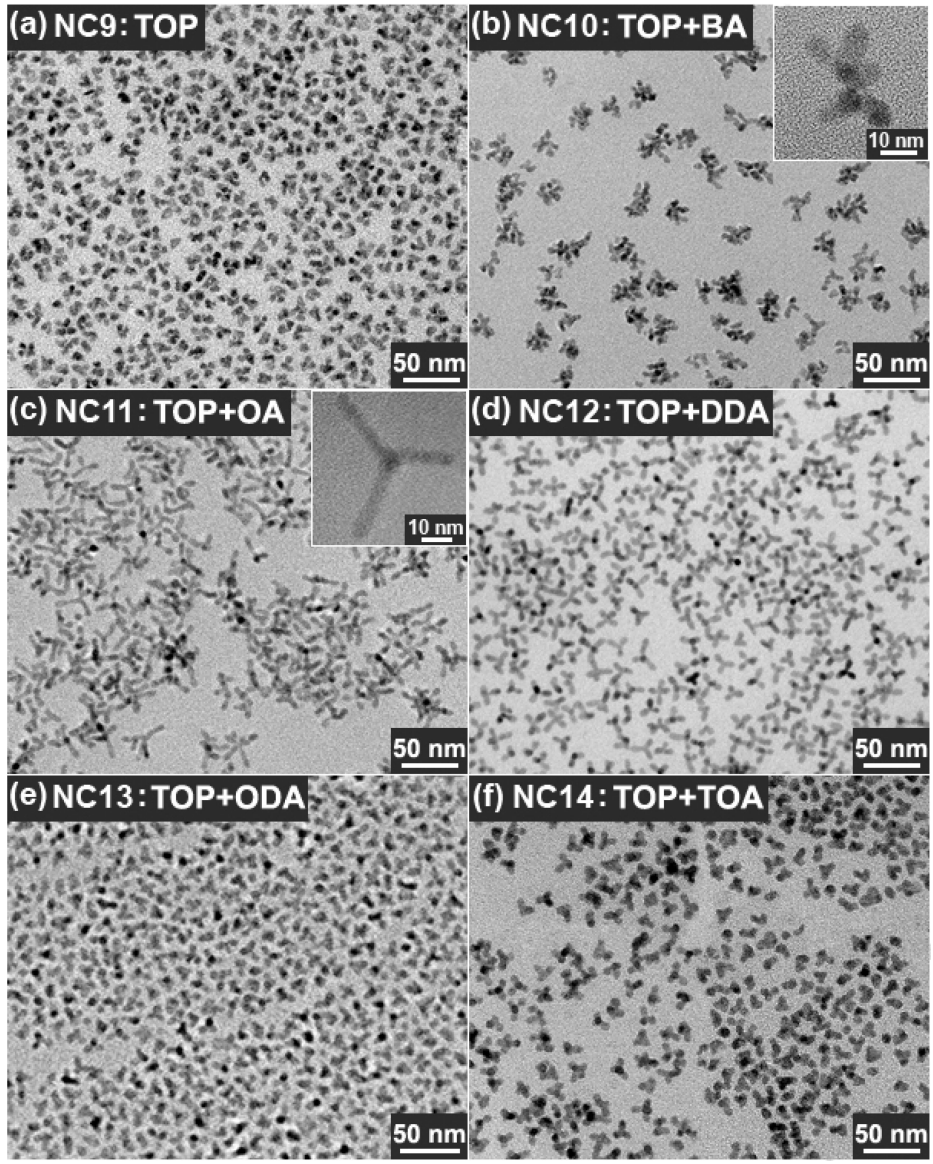

Figure 2. TEM images of CdTe NCs grown using TOP and (a) no amine (NC9), (b) BA (NC10), (c) OA (NC11), (d) DDA (NC12), (e) ODA (NC11), and (f) TOA (NC12).

Table 2. Growth Condition and Shape/Size of the wz-CdTe NCs Attached on CNTs, Synthesized in This Study

					average size of branches[b] (nm)			average size of branches[c] (nm)	
NC	acid[a]	phosphine	amine	shape	*D*	*L*	shape with multi-injection	*D*	*L*
15	OLA	TOP		dot	5 ± 0.5				
16		TOP	OA	tetrapod	5 ± 0.5	12 ± 2			
17	HPA (C6)	TOP		branched (aggregated)[d]	4 ± 0.3	6 ± 1	branched (aggregated)	4 ± 0.3	6 ± 1
18	DPA (C10)	TOP		tetrapod	4 ± 0.2	15 ± 2	tetrapod	4 ± 0.2	20 ± 2
19	TDPA (C14)	TOP		tetrapod	4 ± 0.2	12 ± 2	tetrapod	4 ± 0.2	20 ± 2
20	ODPA (C18)	TOP		dot	3 ± 0.2		tetrapod	3 ± 0.2	25 ± 2

[a] The molar ratio of reactants and ligands is CdO:Te:OLA:TOP:amine = 1:0.5:3.5:2.8:2 and CdO:Te:PA:TOP = 1:1:1.6:10. [b] The average size of branches of CdTe NCs, synthesized using single-injection of Te:TOP; *D* = diameter, *L* = length. [c] The average size of branches of CdTe NCs, synthesized using multi-injection of Te:TOP solution. [d] CdTe NCs are produced as aggregated form.

± 0.3 nm and $L = 6 \pm 1$ nm (inset). A number of these NCs are aggregated to form flower-like nanostructures. The size of the nanoflowers is about 15 nm. The use of DPA (C10) produced longer branched tetrapod-shaped NCs (NC18), as shown in Figure 3d. The average size of the branches increased to $D = 4 \pm 0.2$ nm and $L = 15 \pm 2$ nm. Figure 3e displays the TEM image of the tetrapod shaped CdTe NCs (NC19) synthesized using TDPA. Their average size is $D = 4 \pm 0.2$ nm and $L = 12 \pm 2$ nm. When ODPA was used, the morphology of the CdTe NCs (NC20) approaches that of nanodots with a size of 3 ± 0.2 nm (Figure 3f). The size of the branched tetrapods was maximized when using TDPA.

We monitored the shape evolution of the CdTe NCs, following the multi-injection of the Te precursors, as shown in the Supporting Information, Figure S1. In the case of HPA, the branched morphology (with the same diameter) still

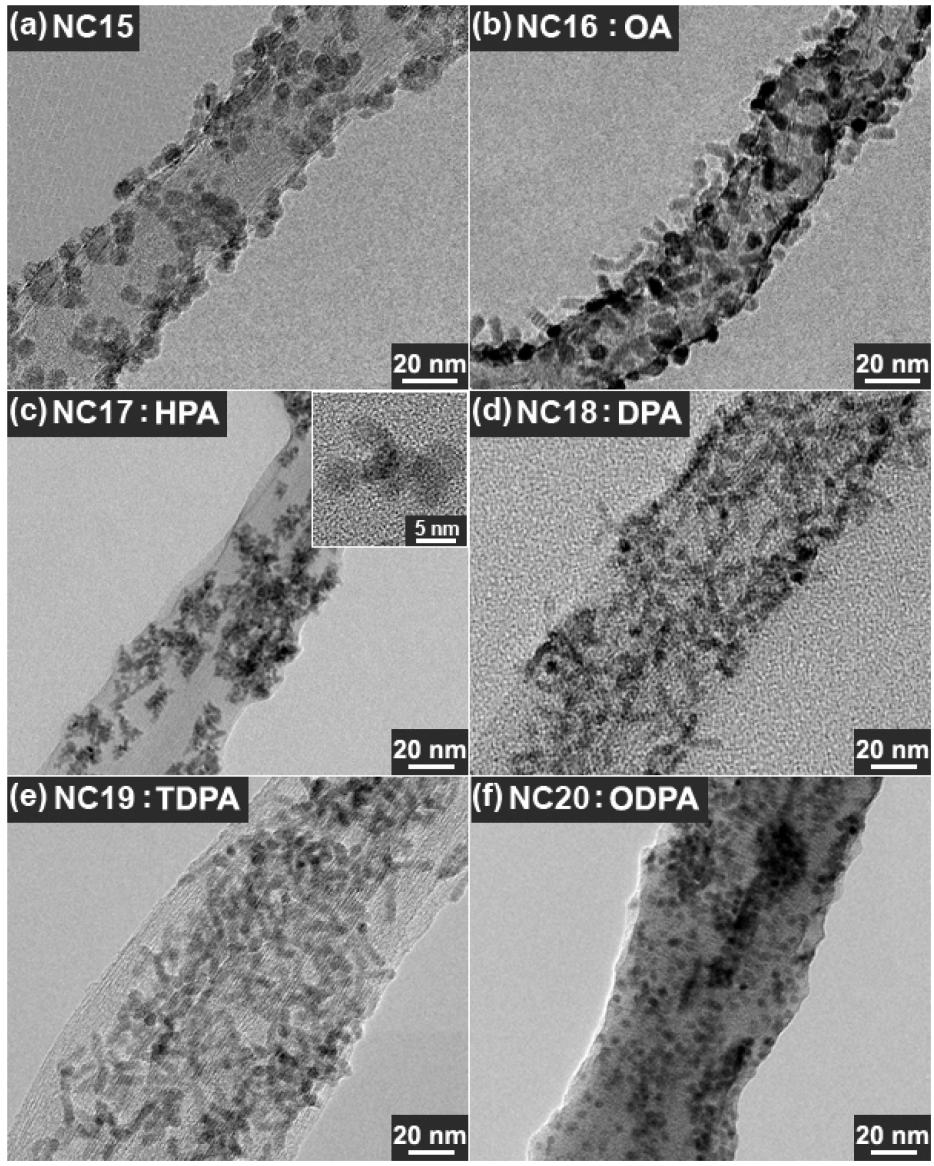

Figure 3. TEM images of CdTe NCs grown on CNTs using (a) no amine (NC15), (b) OA (NC16), (c) HPA (NC17), (d) DPA (NC18), (e) TDPA (NC19), and (f) ODPA (NC20).

remains, but the density of the NCs on the CNTs increases significantly. When DPA and TDPA were used, the length of the tetrapod branches (having the same diameter of 4 ± 0.2 nm) increased to 20 ± 2 nm, upon the multi-injection. In the case of ODPA, the multi-injection induces the formation of tetrapods attached on the SWCNTs with an average size of $D = 3 \pm 0.2$ nm and $L = 25 \pm 2$ nm. The HRTEM and XRD data show the wz-CdTe NCs grown on the CNTs, when using these four phosphonic acids.

3.3. XRD. The XRD measurements reveal that the NC1 and NC9−NC14 consisted of only the zb-CdTe phase, while NC2−NC8 and NC15−NC20 include the wz-CdTe phase. The XRD patterns of NC1, NC3, and NC6, synthesized using TBP, are shown in Figure 4a. The reference peaks of zb-CdTe ($a = 6.481$ Å; JCPDS Card No. 15-0770) and wz-CdTe ($a = 4.58$ Å, $c = 7.50$ Å; JCPDS Card No. 19-0193) are also displayed. The XRD pattern of the dot-shaped NC1 is close to that of the zb-CdTe phase. However, the tetrapod-shaped NC3 and dot-shaped NC6 have a significant degree of wz-CdTe phase. Figure 4b corresponds to the XRD patterns of NC9, NC11, and NC13, synthesized using TOP, showing only zb-CdTe peaks. Figure 4c displays the XRD patterns of NC15, NC17, and NC19, exhibiting consistently the wz-CdTe phase peaks.

3.4. HRTEM Images. The high-resolution TEM (HR-TEM) image of the dot-shaped NC1 shows the zb-CdTe phase (Supporting Information, Figure S2). Figure 5a shows the HRTEM image of a tetrapod-shaped wz-CdTe NC synthesized using TBP and OA (NC3). The image was obtained by projection along the one upward-pointing branch. Its corresponding fast Fourier transform ED (FFT ED) pattern was generated for the branch (marked by (i)) at the zone axis of hexagonal $[01\bar{1}0]$ (inset). The FFT ED pattern of the core part (marked by (ii)) shows the diffraction spots corresponding to the hexagonal [0001] zone axis (inset). The branch consisted of wz-CdTe, grown along the [0001] direction, which is matched to the $[1\bar{1}00]$ direction of the core part. The (002) planes of the branches are consistently

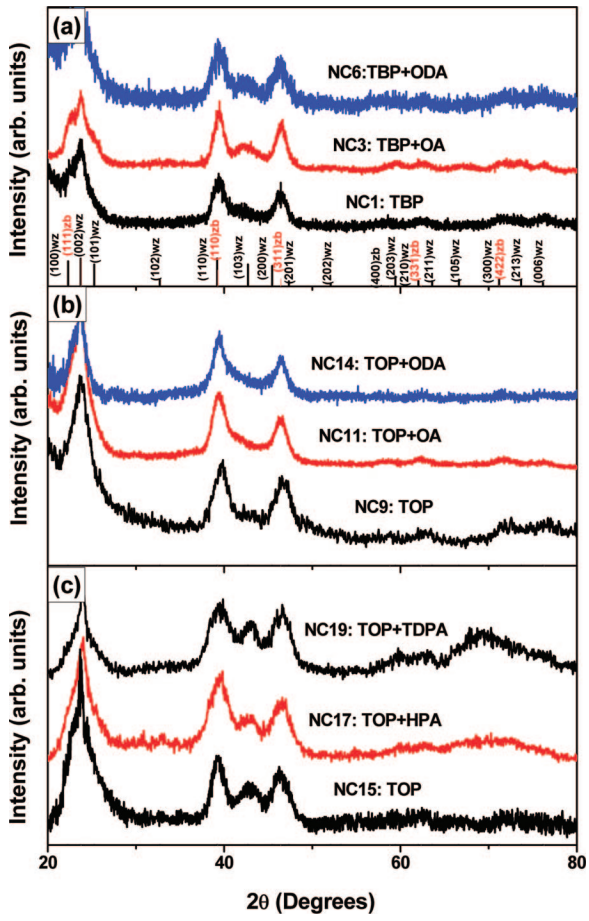

Figure 4. XRD patterns of (a) CdTe reference peaks of zb-CdTe (JCPDS Card No. 15-0770) and wz-CdTe (JCPDS Card No. 19-0193), NC1, NC3, and NC6; (b) NC9, NC11, and NC13; and (c) NC15, NC17, and NC19.

separated by a distance of $d = 3.7$ Å. From this image, it is not easy to identify clearly the phase of the core, since the wz-CdTe branch is projected toward the electron beam. Figure 5b shows the HRTEM image of another tetrapod-shaped CdTe NC (NC3), which is titled with respect to the perpendicular electron beam. In this orientation, the two superimposed branches are oriented in the backward direction (as indicated by the dotted line), and the connection part of the branches with the core is exposed. Its corresponding FFT ED pattern at the hexagonal $[2\bar{1}\bar{1}0]$ zone axis was generated for the branch parts (marked by (i)) and at the cubic [011] zone axis for the core part (marked by (ii)) (insets). The one branch consisted wz-CdTe grown along the [0001] direction, which is matched to the zb-CdTe [111] direction of the core part. The (002) planes of the wz-CdTe branch and the (111) planes of the zb-CdTe core are separated by the same distance of $d = 3.7$ Å. This suggests that the wz-CdTe tetrapod branches, grown along the [0001] direction, are projected along the [111] direction of the zb-CdTe core. It is noteworthy that there are significant stacking faults along the [111] direction of the core part.

Figure 5c shows the HRTEM image of a tetrapod-shaped CdTe NC synthesized using TOP and OA (NC11). For the branch parts, the FFT ED pattern shows the diffraction spots that can be assigned to those of the cubic $[\bar{1}12]$ zone axis (inset). One branch points upward, and the other branch is aligned along the [111] direction. The distance between adjacent (111) planes is $d = 3.7$ Å, which is consistent with that of zb-CdTe. Figure 5d shows the HRTEM image of tetrapod-shaped NCs (NC12), synthesized using TOP and DDA. The two branches are superimposed, as indicated by the dotted line. For both the branch and the core parts, the FFT ED pattern shows the same diffraction spots that can be assigned to those of the cubic [011] zone axis (inset). The growth direction of the individual branches is the [111] direction. The (111) planes are separated by $d = 3.7$ Å, with significant stacking faults. Therefore, the NC11 and NC12 can have zb-CdTe branches that are grown along the [111] direction of the zb-CdTe core. The additional HRTEM images of the zb-CdTe tripod/tetrapods (NC9, NC11, and NC12) are shown in the Supporting Information, Figure S2. The HRTEM images of the NC15, NC16, and NC18 grown on the CNTs are also shown in the Supporting Information, Figure S2.

The UV−visible absorption and PL spectra of CdTe NCs are shown in the Supporting Information, Figure S3. The XPS spectra of the CdTe powders and CdTe NCs are shown in the Supporting Information, Figure S4, confirming the presence of pure and highly crystalline CdTe NCs. The Raman spectra of the CdTe NCs are shown in the Supporting Information, Figure S5. The wz-CdTe tetrapods show a shift of the Raman peaks to a lower frequency than that of the zb-CdTe tetrapods, indicating that there are more defects in the wz-CdTe branched tetrapods.

4. Discussion

4.1. Phase Control of Monodispersed CdTe Tetrapods. A number of works on CdS, CdSe, and CdTe tetrapod NCs demonstrated that they consist of a zb-phase core with four {111} facets, each projecting a wz phase nanorod with a (0001) facet.[10,29,30] It is believed that this polytypism occurs due to the small energy difference between the wz and zb structures and the atomically identical ±{111} facets of the zb and ±(0001) facets of the wz phases.[31] In most of the cases where alkyl phosphonic acids (e.g., TDPA, HDPA, and ODPA) are used as capping ligands, the wz phase growth becomes favored at high growth temperatures. These ligand molecules are known to stabilize the nonpolar lateral facets of the wz-phase NCs. Therefore, the formation of wz-phase branches was induced by the unique "bond strength" and "steric effect" of phosphonic acid toward the elongated nanostructures.

The TEM images of the present CdTe tetrapods suggest that the nucleation occurs in the zb phase, which is consistent

(29) (a) Jun, Y.; Lee, S. M.; Kang, N. J.; Cheon, J *J. Am. Chem. Soc.* **2001**, *123*, 5150. (b) Jun, Y.; Jung, Y.; Cheon, J. *J. Am. Chem. Soc.* **2002**, *124*, 615. (c) Chen, M.; Xie, Y.; Lu, J.; Xiong, Y.; Zhang, S.; Qian, Y.; Liu, X. *J. Mater. Chem.* **2002**, *12*, 748.
(30) (a) Manna, L.; Scher, E. C.; Alivisatos, A. P. *J. Am. Chem. Soc.* **2000**, *122*, 12700. (b) Pang, Q.; Zhao, L.; Cai, Y.; Nguyen, D. P.; Regnault, N.; Wang, N.; Yang, S.; Ge, W.; Ferreira, R.; Bastard, G.; Wang, J. *Chem. Mater.* **2005**, *17*, 5263. (c) Xie, R.; Kolb, U.; Basché, T. *Small* **2006**, *2*, 1454. (d) Asokan, S.; Krueger, K. M.; Colvin, V. L.; Wong, M. S. *Small* **2007**, *3*, 1164.
(31) (a) Yeh, C. -Y.; Lu, Z. W.; Froyen, S.; Zunger, A. *Phys. Rev. B* **1992**, *46*, 10086. (b) Park, C. H.; Cheong, B. H.; Lee, K. -H.; Chang, K. J. *Phys. Rev. B* **1994**, *49*, 4485.

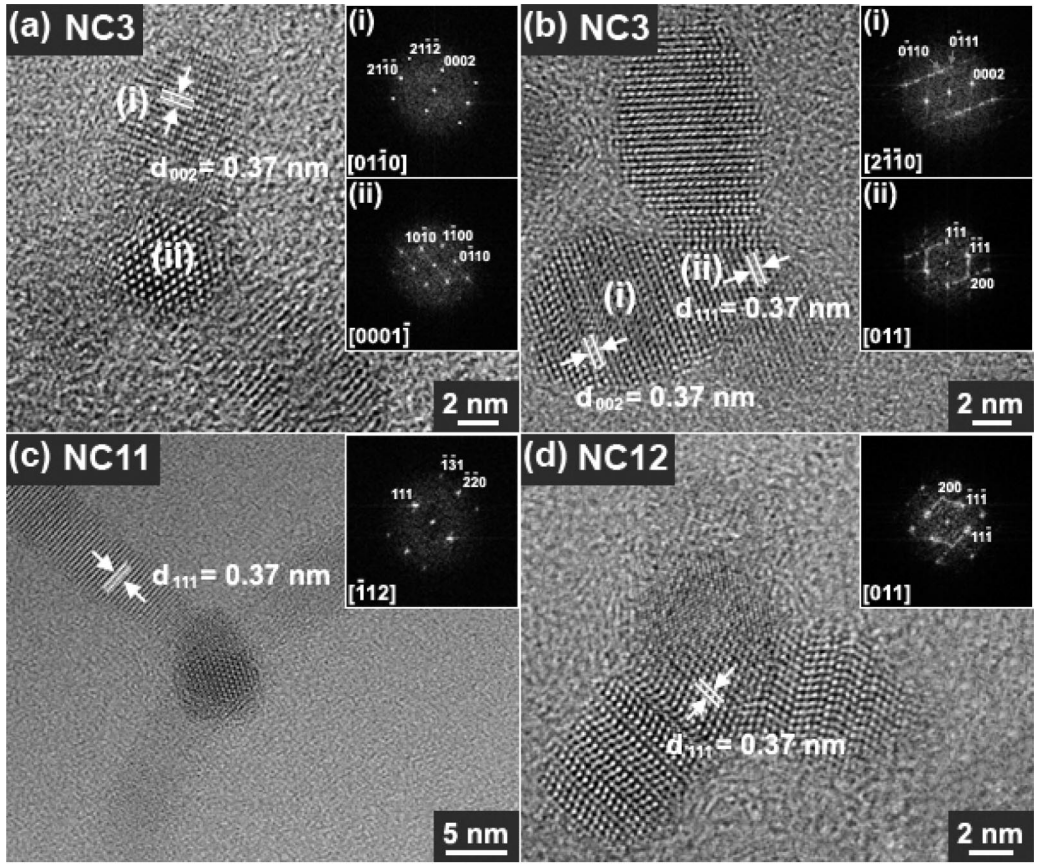

Figure 5. (a) HRTEM image of tetrapod (NC3), with its corresponding FFT ED pattern for the branch (marked by (i)) at the zone axis of hexagonal [01$\bar{1}$0] (inset). FFT ED of core parts (marked by (ii)), generated at the zone axis of hexagonal [0001]. The branch consisted of wz-CdTe, grown along the [0001] direction, which is matched with the [10$\bar{1}$0] direction of the core part. The (002) planes of the branches are separated by $d = 3.7$ Å. (b) HRTEM image of another tetrapod (NC3), with its corresponding FFT ED pattern for the branch (marked by (i)) and core parts (marked by (ii)), at the zone axes of hexagonal [21$\bar{1}$0] and cubic [011], respectively (insets). The hexagonal (002) planes of the branch and the cubic (111) planes of the core are matched with the same distance of $d = 3.7$ Å. (c) HRTEM image of tetrapods (NC11) and the corresponding FFT ED pattern reveal the [111] direction for the individual branches (inset). The distance between adjacent (111) planes is $d = 3.7$ Å. (d) HRTEM image of another type of tetrapod-shaped CdTe NCs (NC12). The FFT ED pattern at the [011] zone axis (for the core and branch parts) shows that the growth direction of the individual branches is the [111] direction. The (111) planes are separated by $d = 3.7$ Å.

with the result of previous works.[10] Remarkably, the four equivalent {111} surfaces of the zb phase core induces the growth of the wz or zb phase branches, depending on the alkyl chain length of phosphine. To the best of our knowledge, this is the first report on the phase control of the tetrapod branches. In the case of CdTe, the zb phase is a thermodynamically stable phase, while the wz phase is a kinetically stable phase that is favored due to the electrostatic interaction between geminal cadmium and tellurium atoms when CdTe monomers approach the crystal surface.[31] As a result of the subtle energy difference (i.e., 8 meV/atom) between the wz- and the zb-CdTe phase, the control of the steric effect of CdTe monomers can have a significant effect on the phase of crystal structure.

A number of works demonstrated that the control of growth regime between kinetic vs thermodynamic growth can be achieved by changing the monomer concentration (activity) at a fixed growth temperature.[12,30a,32] Therefore, we also suggest the following model based on the kinetically or thermodynamically controlled growth of the NCs. For the formation of elongated shapes, a low monomer activity is required in the nucleation stage, while the growth stage requires a high monomer activity.[12] In the presence of TBP and amines, the growth of the wz phase branches is favored by the higher monomer activity at the growth stage, which corresponds to the kinetically controlled growth condition. The more sterically hindered TOP reduces the growth rate by decreasing the monomer activity, and consequently, the more stable zb phase NCs can be grown as branches under the thermodynamically controlled condition. One of critical parameters influencing the growth patterns of NCs is the surface energy of the crystallographic faces of the seed.[33] When sterically less hindered TBP is used as capping ligands, the steric effects on determining the binding geometry of incoming monomers are now minor, and electronic effects play a major role. This facilitates the formation of the kinetically stable wz-CdTe and further induces the formation of rod-shaped NCs (branches) elongated along the *c*-axis under the kinetic growth regime induced by a high monomer concentration. On the other hand, when the more bulky TOP is used, there exists a large steric hindrance between tertiary phosphine capping molecules and the crystal surface. Then the crystal growth of the stable zb phase results under the

(32) Peng, Z. A.; Peng, X. *J. Am. Chem. Soc.* **2001**, *123*, 1389.

(33) Kim, Y.-H.; Jun, Y.; Jun, B.-H.; Lee, S.-M.; Cheon, J. *J. Am. Chem. Soc.* **2002**, *124*, 13656.

thermodynamic growth regime. The phosphine and amine may stabilize the nonpolar lateral facets of both the wz or zb phase branches, and this stabilization considerably reduces the growth rate of these facets. Nevertheless, more advanced models will be necessary to explain the phase control of the CdTe NCs.

4.2. Effects of Amines on the Formation of CdTe Tetrapods. The results also demonstrate strong ligand effects on the shape of CdTe NCs. Peng and co-workers showed that the bonding strength and the steric effect of ligands can affect the reactivity of monomers and determine the shape evolution of CdSe and CdTe NCs.[12,32,34] The ligands are all labile at high temperatures, so the amines, which are strong electron-donating ligands, would be expected to bind to the monomers as coligand and decrease the monomer activity. Herein, the tunable activity of the monomers can be exclusively achieved by varying the alkyl chain of the coligand amines, thus making balanced nucleation and growth possible, which is the key to the control of the size and shape distribution during the synthesis of the monodispersed CdTe NCs.

In the case of TBP, if only OLA was used in a noncoordinating solvent (ODE), the monomer activity (or activity coefficient) was too high, and too many nuclei were formed at the nucleation stage. In this case, the depletion of monomers occurs immediately at the growth stage and, as a result, elongated shapes cannot be formed. When the amines are added, the monomer activity would be expected to decrease as a result of their sufficient ligand protection. The lower consumption of monomers at the nucleation stage increases the monomer activity at the growth stage, and consequently the elongated growth becomes favorable, resulting in the formation of the tetrapods.

The use of BA, whose alkyl chain is the shortest, can increase the monomer activity at the growth stage, thereby inducing the formation of short branched structures. The amines with intermediate chain lengths, OA and DDA, are the best ligands for obtaining the balanced nucleation and growth rate desired for the growth of tetrapods with the longest branches. However, when the alkyl chains become longer than C14, the growth would be inhibited by the excessive steric hindrance. The resultant slower growth rate produces the shorter branched tetrapods during the growth time (10 min). Upon the addition of ODA, the extremely suppressed monomer activity would produce the dot shaped NCs. The bulkier secondary/tertiary alkyl chain of DOA and TOA, as compared to that of the primary alkyl chain of OA, can bind the monomer less strongly and so increases the concentration of nuclei and the depletion rate of the monomers at the growth stage, producing shorter branches, rather than perfect tetrapods. Therefore, we suggest that the morphology evolution from dots to tetrapods can be achieved by controlling the steric hindrance associated with the alkyl chain length of the amines.

The longer alkyl chain of TOP, compared to that of TBP, may increase the degree of ligand protection afforded to the monomers. Assuming that such enhanced ligand protection occurs, the excess TOP would serve as a ligand and its longer alkyl chain might decrease the concentration of nuclei, producing the elongated nanostructures. These results are consistent with the previous observation that TBP yields the dot-shaped NCs, whereas TOP allows the growth of elongated shaped NCs.[35] The addition of OA (and DDA) suppresses the formation of nuclei and increases the monomer activity at the growth stage, generating the well-grown tetrapod structures. The longer branches of the tetrapods than those observed in the case where TBP is used indicates that more balanced growth was achieved for a sufficient reaction time. Similarly to the case of TBP, the steric hindrance of the shorter (BA), longer (ODA), or bulkier alkyl chains (TOA), as compared to those of OA, inhibits the formation of the tetrapods during whole part of the reaction time and decreases the length of the tetrapods.

When BA is used, the branched NCs are aggregated in the case of both TBP and TOP. The flower-like aggregated forms were previously reported for metal oxide (e.g., In_2O_3, CoO, MnO, ZnO), ZnSe, and ZnTe NCs.[36,37] The formation of aggregated forms was demonstrated using the "limited ligand protection" strategy, in which NCs undergo aggregation when the amount of ligands is below the critical concentration necessary for the stabilization of the individual NCs. The short alkyl chains of BA would reduce the degree of surface protection afforded to the CdTe NCs, which provides the increased kinetic driving force needed for their aggregation. The addition of a sufficient amount of longer alkyl chained amines enhances the degree of ligand protection and stabilizes the CdTe NCs in their dispersed form.[37,38]

4.3. Effects of CNTs on the Morphology and Phase of the CdTe NCs. The efficient growth of the CdS and Cu_2S NCs on the CNTs was explained by the lattice matching of the cubic CdS (111) and hexagonal Cu_2S (001) planes with the (002) graphite planes of the CNTs.[21b,28] In the present case, the interlayer distance of the (100) planes of the zb-CdTe (3.24 Å) core matches with that of the (002) graphite planes of the CNTs (3.4 Å), with a small lattice mismatch (5%). The interlayer distances of the (101) and (111) planes of wz-CdTe (3.5 and 2.2 Å) also match with that of the (002) and (100) graphite planes (2.14 Å) of the CNTs, respectively, with a lattice mismatch of 3%. Therefore, this lattice matching may contribute to the high-yield, in situ growth of the CdTe NCs. Furthermore, the surface defect sites of the purified CNTs contain oxygenated functional groups (e.g., −OH or −COOH), which can act as templates and/or ligands for the nucleation and growth of NCs.[23a] The adsorption on the defect sites of the CNTs may increase the monomer activity by eliminating the steric hindrance of the coordinating ligands, thus increasing the concentration of nuclei compared to the growth without CNTs. The increased concentration of nuclei produces the dot-shaped wz-CdTe NCs in the case of both TBP and TOP (as shown in Figure

(34) Jun, Y. W.; Lee, J. H.; Choi, J. S.; Cheon, J. *J. Phys. Chem. B* **2005**, *109*, 14795.

(35) Murray, C. B.; Sun, S.; Gaschler, W.; Doyle, H.; Betley, T. A.; Kagan, C. R. *IBM J. Res. Dev.* **2001**, *45*, 47.

(36) (a) Narayanaswamy, A.; Xu, H.; Pradhan, N.; Peng, X. *Angew. Chem., Int. Ed.* **2006**, *45*, 5361. (b) Narayanaswamy, A.; Xu, H.; Pradhan, N.; Kim, M.; Peng, X. *J. Am. Chem. Soc.* **2006**, *128*, 10310.

(37) Lee, S.; Kim, Y. J.; Park, J. *Chem. Mater.* **2007**, *19*, 4670.

(38) Li, L. S.; Pradhan, N.; Wang, Y.; Peng, X. *Nano Lett.* **2004**, *4*, 2261.

4a). When OA is added, shorter branched tetrapods are produced as compared to those grown without CNTs (as shown in Figure 2c), and the wz-CdTe branches can be favorably formed under kinetically controlled growth conditions, probably as a result of their enhanced growth rates.

To produce efficiently the more elongated tetrapods, another strongly coordinating ligand, alkyl phosphonic acid, was used with the coordinating solvent, TOPO. The present result demonstrates that alkyl phosphonic acid did promote the formation of elongated CdTe NCs, which can be simply explained by the decreased activity of the monomers in the presence of an excessive amount of the weak ligand, TOPO. When HPA was used, the monomer activity was adjusted so as to produce the short branched NCs in the aggregated form. The longer alkyl chain DPA and TDPA decrease the nucleation rate further, due to the steric hindrance of these larger ligands, resulting in the favorable production of the long tetrapod-shaped NCs. The slowest growth rate was achieved using ODPA, which produced the dot-shaped CdTe NCs. HPA serves as an insufficient protection ligand and induces the aggregation of the CdTe NCs into flower-like nanostructures. A sufficient amount of the longer alkyl chained DPA, TDPA, and ODPA would significantly enhance the degree of ligand protection and stabilize the CdTe NCs formed separately on the surface of the CNTs.

Our growth model can be rationalized by the multi-injection of Te precursors. The multi-injection technique is usually used to facilitate the formation of elongated structures. In the case of HPA, the multi-injection increases the density of the aggregated branched NCs without increasing the length of the branches. This indicates that the fast formation of the nuclei makes the elongated shape of the NCs virtually inevitable. The length of the tetrapods increases in the case where multi-injection is used in conjunction with DPA and TDPA. In the case of ODPA, perfect tetrapods were created when multi-injection was performed. This result indicates that the nucleation/growth rate is too slow to form the tetrapods when a single injection was employed. We believe that the multi-injection produces a turbulent increase in the amount of monomers in the reaction solution, thus allowing the growth rate to be efficiently increased. All of the dot and tetrapod shaped CdTe NCs grown on the CNTs consisted of the wz-CdTe structure, due to the enhancement of the nucleation/growth rate as compared to that without the CNTs.

5. Conclusion

High-quality colloidal CdTe NCs were synthesized using CdO, Te, and TBP (or TOP) as the activating agent of Te, OLA as the activating reagent of CdO, and ODE as a noncoordinating solvent. We were able to control the morphology and phase of the CdTe NCs in a simple manner using eight different alkyl-chained amines, BA (C4), OA (C8), DDA (C12), TDA (C14), HDA (C16), ODA (C18), DOA (2 × C8), and TOA (3 × C8), as coligands, without altering the growth temperature or concentration. The evolution of the NCs from spherical dots to tetrapods was achieved. The longest-branched tetrapod shape was obtained in the case of OA (with TOP), where the steric hindrance increases the monomer activity (at the growth stage) sufficiently to grow the tetrapods. The use of TBP (3 × C4) produces the kinetically favorable wz phase branches of the tetrapods, while that of TOP (3 × C8) produces the thermodynamically stable zb phase branches, probably due to the increased steric hindrance of TOP.

The CdTe NCs were grown attached on SWCNTs or MWCNTs, and their shape was successfully controlled using various phosphonic acids instead of OLA and amines, namely, HPA (C6), DPA (C10), TDPA (C14), and ODPA (C18). The longest-branched tetrapod shape becomes dominant for DPA (for single injection), revealing that the steric hindrance of the alkyl chains plays an important role in determining the morphology. This provides important insight into the control of the morphology and phase simply by varying the steric effect of the ligands.

Acknowledgment. This work was supported by KRF grants (R14-2003-033-01003-0; R02-2004-000-10025-0; KRF-2008-314-C00175), KOSEF (R01-2008-000-10825-0; M108030012-1808), KIST (2E20880-08-152), and MKE under the ITRC support program supervised by the IITA (IITA-2008-C1090-0804-0013), and BK21. The SEM, HVEM, XRD, and XPS measurements were performed at the Korea Basic Science Institute at Seoul, Daejeon, Taegu, and Pusan, respectively. The experiments at the PLS were partially supported by MOST and POSTECH.

Supporting Information Available: Additional TEM images, UV−visible absorption and PL spectrum, XPS, and Raman spectra of CdTe NCs (PDF). This material is available free of charge via the Internet at http://pubs.acs.org.

CM801359K